Electronic Structure and Magnetic Anisotropy of an Unsaturated Cyclopentadienyl Iron(I) Complex with 15 Valence Electrons

Chakraborty, U.; Demeshko, S.; Meyer, F.; Rebreyend, C.; de Bruin, B.; Atanasov, M.; Neese, F.; Muehldorf, B.; Wolf, R.

Citation for published version (APA):

Chakraborty, U., Demeshko, S., Meyer, F., Rebreyend, C., de Bruin, B., Atanasov, M., Neese, F., Muehldorf, B., & Wolf, R. (2017). Electronic Structure and Magnetic Anisotropy of an Unsaturated Cyclopentadienyl Iron(I) Complex with 15 Valence Electrons. *Angewandte Chemie, International Edition*, *56*(27), 7995-7999. https://doi.org/10.1002/anie.201702454, https://doi.org/10.1002/ange.201702454

Electronic Structure and Magnetic Anisotropy of an Unsaturated Cyclopentadienyl Iron(I) Complex with 15 Valence Electrons

Uttam Chakraborty, Serhiy Demeshko, Franc Meyer,* Christophe Rebreyend, Bas de Bruin,* Mihail Atanasov,* Frank Neese,* Bernd Mühldorf, and Robert Wolf*
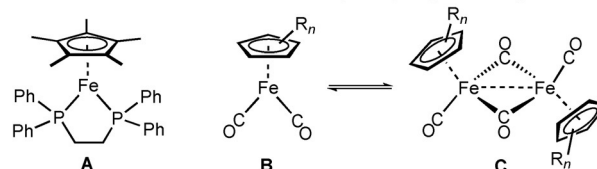
Dedicated to Professor Evamarie Hey-Hawkins on the occasion of her 60th birthday

Abstract: *The 15 valence-electron iron(I) complex [$Cp^{Ar}Fe$-($IiPr_2Me_2$)] (**1**, $Cp^{Ar} = C_5(C_6H_4-4-Et)_5$; $IiPr_2Me_2 = 1,3$-diiso-propyl-4,5-dimethylimidazolin-2-ylidene) was synthesized in high yield from the Fe^{II} precursor [$Cp^{Ar}Fe(\mu-Br)]_2$. ^{57}Fe Mössbauer and EPR spectroscopic data, magnetic measurements, and ab initio ligand-field calculations indicate an $S = 3/2$ ground state with a large negative zero-field splitting. As a consequence, **1** features magnetic anisotropy with an effective spin-reversal barrier of $U_{eff} = 64\ cm^{-1}$. Moreover, **1** catalyzes the dehydrogenation of N,N-dimethylamine–borane, affording tetramethyl-1,3-diaza-2,4-diboretane under mild conditions.*

Decades after cyclopentadienyl iron compounds entered the spotlight,[1,2] this extensive class of compounds continues to fascinate owing to new fundamental insight[3,4] and wide-ranging applications in catalysis and materials science.[5,6] Countless examples make use of ferrocene derivatives.[7]

Mononuclear cyclopentadienyl iron(I) compounds [CpFe-(L_2)] (L being a two-electron donor) are scarce.[8] One example is the [Cp*Fe(dppe)] radical (**A**, Cp* = η^5-C_5Me_5, dppe = 1,2-bis(diphenylphosphino)ethane; Figure 1).[9] While this complex is stable at room temperature as a monomer, related carbonyl complexes [$Cp^RFe(CO)_2$] (**B**, $Cp^R = \eta^5$-C_5H_5 and η^5-C_5Me_5) usually dimerize very rapidly to carbonyl-

[*] Dr. U. Chakraborty, Dr. B. Mühldorf, Prof. Dr. R. Wolf
Institute of Inorganic Chemistry
University of Regensburg, 93040 Regensburg (Germany)
E-mail: robert.wolf@ur.de
Homepage: http://www.uni-regensburg.de/chemistry-pharmacy/
inorganic-chemistry-wolf/index.html

Dr. S. Demeshko, Prof. Dr. F. Meyer
Institute of Inorganic Chemistry
University of Goettingen, 37077 Göttingen (Germany)
E-mail: franc.meyer@chemie.uni-goettingen.de

M. Sc. C. Rebreyend, Prof. Dr. B. de Bruin
Van't Hoff Institute for Molecular Sciences
University of Amsterdam
Science Park 904, 1098 XH Amsterdam (The Netherlands)
E-mail: B.deBruin@uva.nl

Prof. Dr. M. Atanasov, Prof. Dr. F. Neese
Max Planck Institute for Chemical Energy Conversion
Stiftstrasse 34–36, 45470 Mülheim an der Ruhr (Germany)
E-mail: mihail.atanasov@cec.mpg.de
frank.neese@cec.mpg.de

Supporting information and the ORCID identification number(s) for the author(s) of this article can be found under: https://doi.org/10.1002/anie.201702454.

Previous work: 17 valence electron carbonyl and phosphane complexes

This work: 15 valence electron N-heterocyclic carbene complex
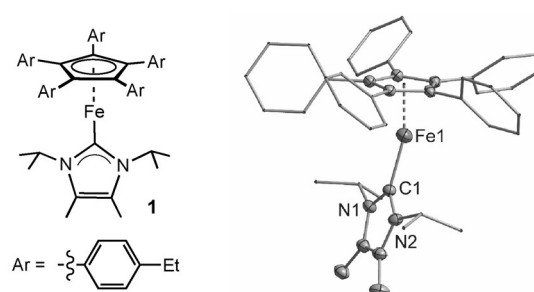
Figure 1. Top: Structural formulae of 17 VE half-sandwich cyclopenta-dienyl iron complexes. Bottom: Structural formula of 15 VE complex **1** and its solid-state molecular structure. For clarity, only one of the two crystallographically independent molecules of **1** is shown. Thermal ellipsoids set at 35% probability. H atoms and ethyl substituents on the aryl rings omitted for clarity. Selected bond lengths [Å] and bond angles [°], the parameters for the second crystallographically independent molecule in the asymmetric unit are given in square brackets: Fe1–C1 1.992(2) [1.996(2)], Fe1–Cp^{Ar}(centroid) 1.851(1) [1.847(1)]; Cp^{Ar}-(centroid)-Fe1-C1 162.11(8) [171.19(8)], Fe1-C1-N1 127.8(2) [128.5(2)], Fe1-C1-N2 127.6(2) [126.6(2)].

bridged complexes **C**.[10,11] Monomer–dimer equilibria were observed even with rather bulky pentaaryl-substituted cyclo-pentadienyl ligands [$Cp^R = \eta^5$-C_5Ph_5, η^5-C_5Ph_4(p-tolyl), and η^5-$C_5(C_6H_4$-4-$nBu)_5$].[10,12] The pentaisopropyl-substituted complex [(η^5-C_5iPr_5)$Fe(CO)_2$] is a monomer in solution, but forms a carbonyl-bridged dimer in the solid state.[13]

Stable 15 valence electron (VE) iron(I) species of the type [$Cp^RFe(L)$] appear to be unknown.[14–16] IR spectroscopic studies suggested the formation of a triply bonded species [$Cp(CO)Fe \equiv Fe(CO)Cp$] by stepwise decarbonylation of [$CpFe(CO)_2]_2$ in a 3-methylpentane matrix at 98 K,[15] while prolonged heating of [$CpFe(CO)_2]_2$ in xylene led to the tetrahedral cluster [$Cp_4Fe_4(CO)_4$].[16] Herein, we report the synthesis of a 15 VE cyclopentadienyl iron(I) complex [$Cp^{Ar}Fe(IiPr_2Me_2)$] (**1**, $IiPr_2Me_2 = 1,3$-diisopropyl-4,5-dime-thylimidazol-2-ylidene). Spectroscopic studies, magnetic measurements, and quantum-chemical calculations revealed

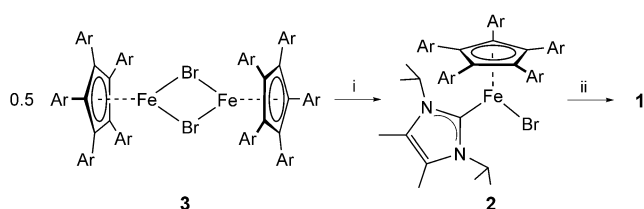**Scheme 1.** Synthesis of **1**; Ar = C$_6$H$_4$-4-Et. Reagents and conditions: i) addition of IiPr$_2$Me$_2$, benzene, RT; ii) addition of KC$_8$ and benzene, loss of KBr and graphite.

a pronounced magnetic anisotropy for **1**, a property required for single-molecule magnets (SMMs).[17–19]

Complex **1** was isolated in 78% yield by reducing [Cp^{Ar}FeBr(IiPr$_2$Me$_2$)] (**2**), which had been prepared in situ from [Cp^{Ar}Fe(μ-Br)]$_2$ (**3**, Cp^{Ar} = C$_5$(C$_6$H$_4$-4-Et)$_5$) and IiPr$_2$Me$_2$ (Scheme 1), with potassium graphite in benzene over two days.[20] Broad ^{1}H NMR resonances were observed in C$_6$D$_6$ solution between −36 and 61 ppm (Figure S1 in the Supporting Information). Single-crystal X-ray diffraction revealed the slightly bent "pogo-stick" structure of **1** (Figure 1) with an η^5-coordinated Cp^{Ar} ligand and Cp^{Ar}(centroid)-Fe-C$_{carbene}$ angles of 162.11(8)° and 171.19(8)° for two crystallographically independent molecules in the unit cell. The Fe–Cp^{Ar}-(centroid) distance [1.851(1) and 1.847(1) Å] is shorter than in **2** [2.038(1) and 2.020(1) Å for two crystallographically independent molecules]. The Fe−C$_{carbene}$ bonds (1.992(2) and 1.996(2) Å) are similar in length to the Fe−C$_{carbene}$ bond of 2.014(2) Å for two-coordinate [(IPr)Fe^I(N{SiMe$_3$}Dipp)] (Dipp = C$_6$H$_3$-2,6-iPr$_2$),[21] and the Fe−C$_{carbene}$ bonds of 2.110(3) and 2.128(3) Å observed for Fe^{II} complex **2**. Dark-yellow **1** is paramagnetic, thermally stable, and air-sensitive as a solid. A magnetic moment of μ_{eff} = 5.4(1) μ_B was determined in C$_6$D$_6$ solution using the Evans method.

Linear two-coordinate Fe^{II} (d^6) and Fe^I (d^7) complexes possess ^{5}E and ^{4}E electronic ground states and therefore have unquenched orbital momenta.[22–37] Spin–orbit coupling leads to orbital moment contributions to the S = 2 and S = 3/2 spins. Therefore, some orientations of the magnetic moment will be strongly preferred (magnetic anisotropy). We were keen to study how the unsymmetric structure that arises from the specific ligand set of **1** affects the electronic structure and the magnetic behavior.

Temperature-dependent magnetic susceptibility and variable-temperature/variable-field (VTVH) magnetization measurements (Figure S12) support an S = 3/2 spin ground state, with best fit values of $g_x = g_y$ = 2.18, g_z = 2.52, D = −33.4 cm^{-1}, and E/D = 0. The large negative zero-field splitting parameter D indicates that at low temperatures, only the Kramers doublet with $m_s = \pm 3/2$ is populated, which is a prerequisite for Fe^I-based SMMs.

A first indication for the SMM-type behavior of **1** came from Mössbauer spectra (Figure S16), which are in line with a large unquenched orbital magnetic moment at low temperature. The spectrum at 80 K is unsymmetrically broadened, indicating the onset of slow paramagnetic relaxation on the Mössbauer time scale (ca. 10^{-7} s).[38] At 7 K, this leads to a sharp octet, which could be simulated with a spin Hamil-

tonian calculation for an effective spin of S = 3/2 and a uniaxial internal magnetic field on the iron nucleus of H_{int} = 16.1 T.

Alternating current (AC) magnetic susceptibility measurements in the absence of a direct current (DC) magnetic field (Figure S13) revealed a characteristic out-of-phase signal even though the characteristic maxima in the imaginary part (χ'') were not observed, which is presumably due to barrierless quantum tunneling of magnetization enabled by the bent structure of **1**. The application of DC fields of ≥ 1000 Oe (Figure S14), which suppress quantum tunneling, led to the clear observation of frequency-dependent maxima of χ'' (Figure 2). Analysis of the temperature-dependent χ''
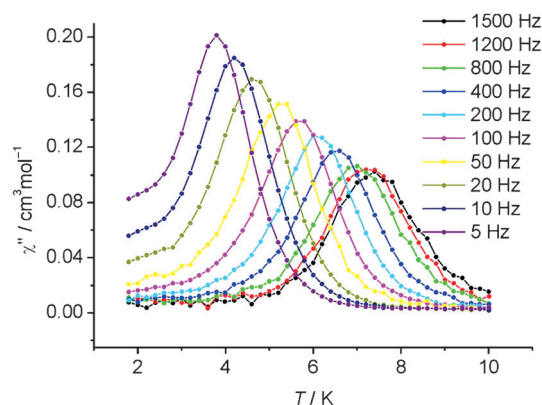

Figure 2. Temperature dependence of χ'' for **1** at various frequencies with an applied DC field of H_{dc} = 1000 Oe.

data (Figure S15) taking into account Raman and Orbach relaxation mechanisms[42] revealed an energy barrier of U_{eff} = 63.6 cm^{-1} and a characteristic relaxation time of τ_0 = 6.8 × 10^{-10} s. The calculated U_{eff} parameter (63.6 cm^{-1}) is in good agreement with the value estimated from DC susceptibility measurements ($|2D|$ = 67 cm^{-1}).

To probe the electronic structure and the magnetic properties of **1**, we carried out complete active space self-consistent field (CASSCF) and n electron valence state perturbation theory to second order (NEVPT2) calculations on the crystallographically determined molecular structure (see the Supporting Information). By using the recently developed ab initio ligand field theory (AILFT),[39] the Racah parameters B and C and the spin–orbit coupling parameter ζ were calculated. The Cp^{Ar} and N-heterocyclic carbene (NHC) donors and the considerable tilting of the cyclopentadienyl ligand (Cp-Fe-C angle 166.6°) lead to a modification of the electronic structure (Figure 3a) compared with an ideal linear MX$_2$ complex:

i) The NHC ligand features out-of-plane electrons that are available for π-bonding but no such electrons in the ligand plane. This π-anisotropy leads to a splitting of the d$_{xz}$,d$_{yz}$ orbital pair, which would otherwise be degenerate.

ii) Bending of the Cp-Fe-C vector from linearity induces a splitting of the 3d$_{xy}$,3d$_{x^2-y^2}$ orbital pair owing to indirect (via their mixing with 3d$_{xz,yz}$) σ- and π-overlap with ligand orbitals, which becomes non-zero for C-Fe-C deviating from linearity.
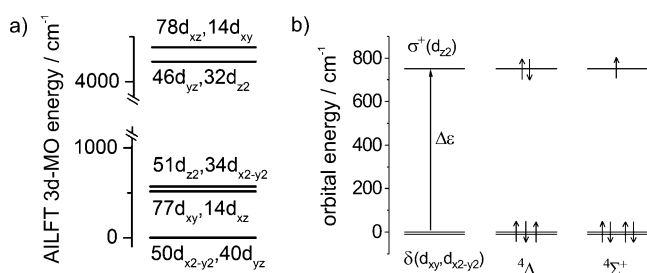
Figure 3. a) AILFT (NEVPT2) ligand-field diagram for **1** with leading 3d MO contributions for Fe. b) Orbital splitting and electronic configurations for the ground state ($^4\Delta$, energy at 0) and the $^4\Sigma^+$ excited state (energy at $12B-\Delta\varepsilon$) of **1** following holohedrization of the ligand field matrix from the reported C_1 to $C_{\infty v}$ point symmetry; the diagram has been plotted using parameter values of $B = 722\ cm^{-1}$ and $\Delta\varepsilon = 751\ cm^{-1}$ as derived using the procedure elaborated in the Supporting Information. The orbitals d_{xz} and d_{yz}, which are singly occupied in both states, were computed at $1979\ cm^{-1}$ and are not shown.

iii) Large 3d–4s mixing is evident from the very low energy of the MO of d_{z^2} character. This is due to metal–ligand interactions, which place this MO just above the $3d_{xy}$ MO.

iv) The low symmetry induces extensive 3d MO mixing.

Taken together, these effects (i–iv) lead to an unusual configuration of the 3d orbitals in the (non-relativistic, spin-free) ground state. In addition, interelectronic repulsion energetically favors a non-aufbau electron distribution in the ground state as shown in Figure 3b for complex **1** following a symmetrization of the ligand field from the reported C_1 to the holohedral symmetry $C_{\infty v}$ (see the Supporting Information for details regarding the procedure). The aufbau occupation $d_{x^2-y^2}^2 d_{xy}^2 d_{z^2}^1 d_{xz}^1 d_{yz}^1$ corresponds to an excited state that is disfavored in energy by $12B = 8664\ cm^{-1}$ ($B = 722\ cm^{-1}$) with respect to the $^4\Delta$ ground state. This large energy by far exceeds the $d_{z^2} - d_{x^2-y^2} d_{xy}$ orbital energy difference of $\Delta\varepsilon = 751\ cm^{-1}$.

The $S = 3/2$ ground state additionally splits into two separate Kramers doublets, $|m_s\rangle = |\pm 1/2\rangle$ and $|\pm 3/2\rangle$, through spin–orbit coupling. The $|m_s\rangle = |\pm 3/2\rangle$ Kramers doublet is the magnetic ground state owing to the negative zero-field splitting parameters $D = -42\ cm^{-1}$ and $E = -0.50\ cm^{-1}$. The experimental value ($D = -33.4\ cm^{-1}$, see above) is somewhat smaller, presumably owing to vibronic coupling. Large orbital contributions to the effective magnetic moment are apparent from the calculated effective g-tensor values with dominant axial (Ising-type) anisotropy for the ground-state Kramers doublet ($g_z, g_x, g_y = 8.362, 0.075, 0.075$) and easy plane anisotropy for the excited Kramers doublet ($g_z, g_x, g_y = 2.955, 4.056, 4.182$). These can be compared with the computed intrinsic spin Hamiltonian values of $g_z, g_x, g_y = 2.802, 2.080, 2.067$.

The results of the calculations are consistent with our EPR spectroscopic data for **1**. The $\Delta m_s = 3$ transition within the magnetic $|m_s\rangle = |\pm 3/2\rangle$ ground-state doublet is formally forbidden, and hence associated with a very weak EPR signal intensity. Accordingly, X-band EPR measurements at 30 K using a microwave power of about 1 mW merely showed

the signals of a minor $S = 1/2$ impurity ($< 0.1\%$ of the total Fe concentration according to spin integration measurements, see Figure S17). Only in spectra recorded with a higher microwave power (200 mW) and at a lower temperature (8 K), a derivative signal consisting of a single, relatively sharp low-field peak at $g_{eff} = 7.76$ became visible (Figure S18), which corresponds to the main $S = 3/2$ species. This signal can be assigned to the resonance stemming from the z-component of the very anisotropic $g_{eff}^{\pm 3/2}$ tensor of the $|\pm 3/2\rangle$ Kramers doublet. With a sufficiently large zero-field splitting relative to the microwave energy ($h\nu \approx 0.3\ cm^{-1}$ for X-band), the effective g-value (g_{eff}) of the $g_z^{\pm 3/2}$ signal should depend only on the rhombicity parameter E/D and the real g_z-value of the $S = 3/2$ species.[40] The deviation of the measured effective g_z-value from the expected value of six thus shows that the g-tensor of the $S = 3/2$ system indeed has a z-component that is significantly larger than two. Based on the near-zero rhombicity parameter ($E/D \approx 0$) found by the magnetic measurements and the calculations, a reasonable value of $g_z \approx 2.55$ can be estimated from spectral simulations, thus reproducing the position of the experimentally observed EPR signal at $g_{eff} = 7.76$. This value compares well with the value of $g_z = 2.6$ reported for $[(nacnac)Fe^I(AdNNNNAd)]$ $[nacnac = HC\{C-(Me)N(C_6H_3-2,6-iPr_2)\}_2]$, which also has an $S = 3/2$ ground state with a large negative zero-field splitting, $D < 0$.[40]

The SMM-type behavior of **1** is unusual given the unsymmetric, non-linear molecular structure.[17,21–37] Several linear Fe^I and Fe^{II} complexes have been reported to feature large unquenched orbital contributions to the magnetic moment.[21–27,29–31,34–37] A few of these have SMM properties. For example, the Fe^{II} complex $[(C_5iPr_5)Fe(C_6H_3-2,6-iPr_2)]$, which has a linear structure, does not show slow magnetic relaxation in the absence of an applied field owing to fast quantum tunneling of magnetization,[25] but a spin-reversal barrier of $U_{eff} = 28.1\ cm^{-1}$ was determined in a DC field of 750 Oe. Similar spin-reversal barriers were determined for linear Fe^I species, for example, $[K(L)][Fe^I\{N(SiMe_3)_2\}_2]^-$ (L = [18]crown-6 and [2.2.2.]crypt, $U_{eff} = 43$ and $64\ cm^{-1}$),[37] trigonal-planar $[(CAAC)_2Fe^ICl]$ ($U_{eff} = 22.4\ cm^{-1}$),[34] $[Fe^{II}\{N-(SiMe_3)_2\}_2(PCy_3)]$,[26,32] and the tetrahedral complex $[(PNP)Fe^{III}Cl_2]$ ($PNP^- = N[2-P(CHMe_2)_2-4-methylphenyl]_2^-$, $U_{eff} = 32–26\ cm^{-1}$).[28] Significantly, the highest spin-reversal barrier reported for any Fe-based SMM was observed for $[K(crypt-222)][Fe^I\{C(SiMe_3)_3\}_2]$ (**D**, $U_{eff} = 264\ cm^{-1}$), which has axial D_{3d} symmetry and a ^4E ground state.[30] As a consequence, **D** shows magnetic hysteresis and blocking of the magnetization at temperatures below 4.5 K.

Why is the spin-reversal barrier in **1** smaller than that in **D**? To address this question, we performed calculations on the model complex $[Fe(CH_3)_2]^-$ (see the Supporting Information), which has a D_{3d} symmetric structure. Compared to **1**, **D** has higher ground-state anisotropy ($g_z = 10$ in $[Fe(CH_3)_2]^-$, $g_z = 8.4$ in **1**) and a larger energy separation between the ground and the lowest excited Kramers doublet (224 cm^{-1} in $[Fe(CH_3)_2]^-$, 84 cm^{-1} in **1**). However, the most striking difference is the direct relaxation pathway predicted to be available in **1**. As shown by Figure 4, the transitions from the ground state to the excited states are accompanied by sizable horizontal pathways (usually referred to as quantum tunnel-
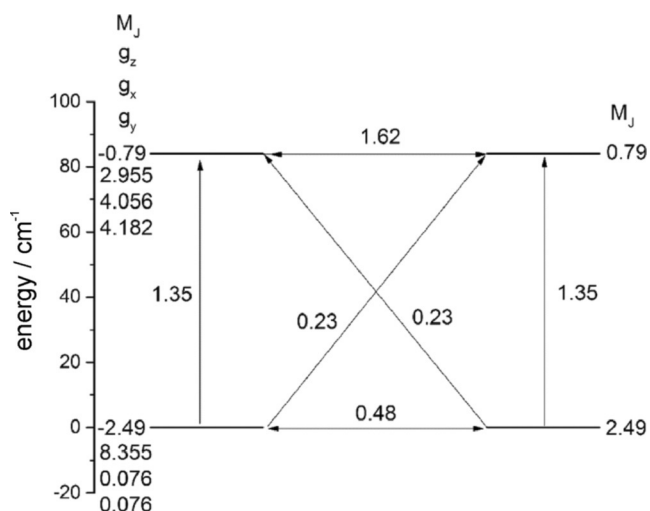
Figure 4. Effective M_J and main g-tensor components for the ground and first excited states of **1**. The arrows and the corresponding numbers describe matrix elements for magnetic dipolar transitions of relevance for the magnetic relaxation.

ing of magnetization); these are larger for the excited state (1.62) and smaller, yet non-negligible (0.48), for the ground state. Unlike the vertical transitions, which require an absorption (emission) of vibrational quanta that is hardly accomplished at cryogenic temperatures, horizontal transitions provide a pathway for magnetic relaxation in **1**. In particular, direct transitions between the ground-state sublevels are expected to dominate for temperatures of 2 to 10 K. For $[Fe(CH_3)_2]^-$, we did not observe horizontal relaxation because with the high D_{3d} symmetry and without vibrations lifting the center of inversion, there is no transversal anisotropy that can assist the reversal of the magnetic moment (Figure S19).

In an initial study of the reactivity and the catalytic properties of **1**, we found that this complex does not react with H_2 and N_2 under ambient conditions, but it is an active (pre)catalyst for the dehydrogenation of *N,N*-dimethylamine–borane (DMAB).[43–48] This reaction came to our attention through a recent report by Manners and co-workers, who used the carbonyl complexes $[CpFe(CO)_2I]$, $[CpFe(CO)_2]_2$, and $[Cp_2Fe_2(CO)_3(CH_3CN)]$ as catalyst precursors.[43] In the presence of **1** (5 mol%), DMAB was completely converted within 7 h into tetramethyl-1,3-diaza-2,4-diboretane (**4**) and bis(dimethylamino)borane (**5**), which were formed in a 9:1 ratio according to ^{11}B NMR spectroscopy (Scheme 2 and Figures S3–S5). Tetramethyl-1,3-diborazane **6** was detected as an intermediate. Catalyst **1** remained active after conversion was complete as shown by the addition of fresh substrate (Figures S9 and S10). Quantitative poisoning studies with $P(OMe_3)$ and dibenzo[*a,e*]cyclooctatetraene (DCT) point towards a homogeneous mechanism (Scheme 2, see the Supporting Information for details).

In summary, we have synthesized the first 15 VE cyclopentadienyl iron(I) complex **1**, which is a rare organometallic iron complex with a heteroleptic structure and the properties of a single-molecule magnet.[17,18] The basis for the SMM behavior is the unusual electronic structure, where extensive
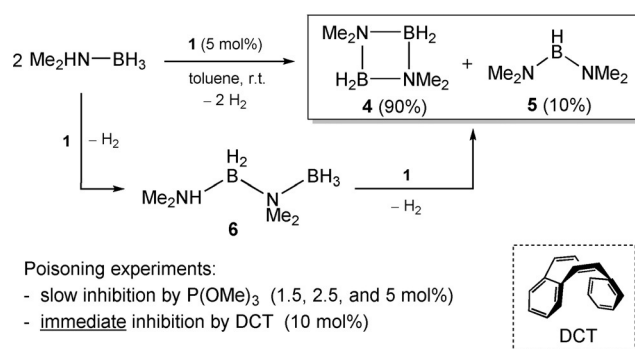
Scheme 2. Catalytic dehydrogenation of *N,N*-dimethylamine–borane in the presence of **3**.

metal–ligand interactions and 3d–4s mixing that are due to the bent structure produce a nearly orbitally degenerate ground state. As a consequence, **1** shows slow relaxation of the magnetization in the presence and even in the absence of an external magnetic field. Furthermore, **1** catalyzes dimethylamine–borane dehydrogenation, a reaction for which only a few other iron catalysts are known.[43–48] This initial result bodes well for the future development of further synthetic and catalytic applications of **1** and related cyclopentadienyl iron(I) complexes.

Acknowledgements

Conflict of interest

The authors declare no conflict of interest.

[1] a) T. J. Kealy, P. L. Pauson, *Nature* **1951**, *168*, 1039; b) S. A. Miller, J. A. Tebboth, J. F. Tremaine, *J. Chem. Soc.* **1952**, 632; c) G. Wilkinson, M. Rosenblum, M. C. Whiting, R. B. Woodward, *J. Am. Chem. Soc.* **1952**, *74*, 2125.

[2] For a review, see: H. Werner, *Angew. Chem. Int. Ed.* **2012**, *51*, 6052; *Angew. Chem.* **2012**, *124*, 6156.

[3] M. Malischewski, M. Adelhardt, J. Sutter, K. Meyer, K. Seppelt, *Science* **2016**, *353*, 678.

[4] M. S. Inkpen, S. Scheerer, M. Linseis, A. J. P. White, R. F. Winter, T. Albrecht, N. J. Long, *Nat. Chem.* **2016**, *8*, 825.

[5] *The Chemistry of Organoiron Compounds* (Eds.: I. Marek, Z. Rappoport), Wiley, Hoboken, **2014**.

[6] I. Bauer, H.-J. Knölker, *Chem. Rev.* **2015**, *115*, 3170.

[7] a) *Metallocenes* (Eds.: A. Togni, R. L. Halterman), Wiley-VCH, Weinheim, **2008**; b) R. Peters, D. F. Fischer, S. Jautze, *Top. Organomet. Chem.* **2011**, *33*, 139.

[8] M. C. Baird, *Chem. Rev.* **1988**, *88*, 1217.

[9] P. Hamon, L. Toupet, J.-R. Hamon, C. Lapinte, *Organometallics* **1996**, *15*, 10.

[10] a) B. D. Moore, M. B. Simpson, M. Poliakoff, J. J. Turner, *J. Chem. Soc. Chem. Commun.* **1984**, 972; b) B. D. Moore, M. Poliakoff, J. J. Turner, *J. Am. Chem. Soc.* **1986**, *108*, 1819; c) P. E. Bloyce, A. K. Campen, R. H. Hooker, A. J. Rest, N. R. Thomas, T. E. Bitterwolf, J. E. Shade, *J. Chem. Soc. Dalton Trans.* **1990**, 2833; d) A. J. Dixon, M. W. George, C. Hughes, M. Poliakoff, J. J. Turner, *J. Am. Chem. Soc.* **1992**, *114*, 1719.

[11] a) I. Kuksis, M. C. Baird, *Organometallics* **1994**, *13*, 1551; b) I. Kuksis, M. C. Baird, *Organometallics* **1996**, *15*, 4755, and references therein.

[12] S. Heinl, G. Balázs, M. Scheer, *Phosphorus Sulfur Silicon Relat. Elem.* **2014**, *189*, 924.

[13] H. Sitzmann, T. Dezember, W. Kaim, F. Baumann, D. Stalke, J. Kärcher, E. Dormann, H. Winter, C. Wachter, M. Kelemen, *Angew. Chem. Int. Ed. Engl.* **1996**, *35*, 2872; *Angew. Chem.* **1996**, *108*, 3013.

[14] 17 VE Ni^I complexes $[Cp^{Ar}Ni(L)]$ were recently reported by some of us [L = IPr (1,3-bis(2,6-diisopropylphenyl)imidazol-2-ylidene), $IiPr_2Me_2$, and Ga(nacnac)]; see: a) U. Chakraborty, F. Urban, B. Mühldorf, C. Rebreyend, B. de Bruin, N. van Velzen, S. Harder, R. Wolf, *Organometallics* **2016**, *35*, 1624; b) U. Chakraborty, B. Mühldorf, N. J. C. van Velzen, B. de Bruin, S. Harder, R. Wolf, *Inorg. Chem.* **2016**, *55*, 3075.

[15] F. A. Kvietok, B. E. Bursten, *J. Am. Chem. Soc.* **1994**, *116*, 9807, and references therein.

[16] a) R. B. King, *Inorg. Chem.* **1966**, *5*, 2227; b) M. A. Neuman, Trinh-Toan, L. F. Dahl, *J. Am. Chem. Soc.* **1972**, *94*, 3383.

[17] After this paper had been submitted, Walter and co-workers independently reported the closely related trialkyl-substituted cyclopentadienyl compound $[Cp^{tBu_3}Fe(IiPr_2Me_2)]$ ($Cp^{tBu_3} = \eta^5$-1,2,4-$(Me_3C)_3C_5H_2$).[18] An axial splitting parameter of $D = -16.4\ cm^{-1}$ (with $E/D = 0$) was determined for this complex based on magnetic measurements and ^{57}Fe Mössbauer studies. In contrast to **1**, $[Cp^{tBu_3}Fe(IiPr_2Me_2)]$ reversibly binds N_2, forming the 17 VE species $[Cp^{tBu_3}Fe(IiPr_2Me_2)(\eta^1-N_2)]$.

[18] M. Reiners, D. Baabe, M.-K. Zaretzke, M. Freytag, M. D. Walter, *Chem. Commun.* https://doi.org/10.1002/c7cc01535f.

[19] For reviews on single-molecule magnetism, see: a) R. A. Layfield, *Organometallics* **2014**, *33*, 1084; b) G. A. Craig, M. Murrie, *Chem. Soc. Rev.* **2015**, *44*, 2135; c) S. Gómez-Coca, D. Aravena, R. Morales, E. Ruiz, *Coord. Chem. Rev.* **2015**, *289–290*, 379; d) A. K. Bar, C. Pichon, J.-P. Sutter, *Coord. Chem. Rev.* **2016**, *308*, 346; e) J. M. Frost, K. L. M. Harriman, M. Murugesu, *Chem. Sci.* **2016**, *7*, 2470.

[20] For the related alkyl-substituted complex $[Cp^{tBu_3}FeI(IiPr_2Me_2)]$, see: M. Reiners, D. Baabe, K. Harms, M. Maekawa, C. G. Daniliuc, M. Freytag, P. G. Jones, M. D. Walter, *Inorg. Chem. Front.* **2016**, *3*, 250.

[21] M. I. Lipschutz, T. Chantarojsiri, Y. Dong, T. D. Tilley, *J. Am. Chem. Soc.* **2015**, *137*, 6366.

[22] W. M. Reiff, A. M. LaPointe, E. H. Witten, *J. Am. Chem. Soc.* **2004**, *126*, 10206.

[23] W. A. Merrill, T. A. Stich, M. Brynda, G. J. Yeagle, J. C. Fettinger, R. D. Hont, W. M. Reiff, C. E. Schulz, R. D. Britt, P. P. Power, *J. Am. Chem. Soc.* **2009**, *131*, 12693.

[24] W. M. Reiff, C. E. Schulz, M.-H. Whangbo, J. I. Seo, Y. S. Lee, G. R. Potratz, C. W. Spicer, G. S. Girolami, *J. Am. Chem. Soc.* **2009**, *131*, 404.

[25] D. Weismann, Y. Sun, Y. Lan, G. Wolmershäuser, A. K. Powell, H. Sitzmann, *Chem. Eur. J.* **2011**, *17*, 4700.

[26] P.-H. Lin, N. C. Smythe, S. I. Gorelsky, S. Maguire, N. J. Henson, I. Korobkov, B. L. Scott, J. C. Gordon, R. T. Baker, M. Murugesu, *J. Am. Chem. Soc.* **2011**, *133*, 15806.

[27] M. Atanasov, J. M. Zadrozny, J. R. Long, F. Neese, *Chem. Sci.* **2013**, *4*, 139.

[28] S. Mossin, B. L. Tran, D. Adhikari, M. Pink, F. W. Heinemann, J. Sutter, R. K. Szilagyi, K. Meyer, D. J. Mindiola, *J. Am. Chem. Soc.* **2012**, *134*, 13651.

[29] J. M. Zadrozny, M. Atanasov, A. M. Bryan, C.-Y. Lin, B. D. Rekken, P. P. Power, F. Neese, J. R. Long, *Chem. Sci.* **2013**, *4*, 125.

[30] J. M. Zadrozny, D. J. Xiao, M. Atanasov, G. J. Long, F. Grandjean, F. Neese, J. R. Long, *Nat. Chem.* **2013**, *5*, 577.

[31] J. M. Zadrozny, D. J. Xiao, J. R. Long, M. Atanasov, F. Neese, F. Grandjean, G. J. Long, *Inorg. Chem.* **2013**, *52*, 13123.

[32] A. Eichhöfer, Y. Lan, V. Mereacre, T. Bodenstein, F. Weigend, *Inorg. Chem.* **2014**, *53*, 1962.

[33] C.-Y. Lin, J. C. Fettinger, F. Grandjean, G. J. Long, P. P. Power, *Inorg. Chem.* **2014**, *53*, 9400.

[34] P. P. Samuel, K. C. Mondal, N. Amin Sk, H. W. Roesky, E. Carl, R. Neufeld, D. Stalke, S. Demeshko, F. Meyer, L. Ungur, L. F. Chibotaru, J. Christian, V. Ramachandran, J. van Tol, N. S. Dalal, *J. Am. Chem. Soc.* **2014**, *136*, 11964.

[35] G. Ung, J. Rittle, M. Soleilhavoup, G. Bertrand, J. C. Peters, *Angew. Chem. Int. Ed.* **2014**, *53*, 8427; *Angew. Chem.* **2014**, *126*, 8567.

[36] A. K. Bar, C. Pichon, N. Gogoi, C. Duhayon, S. Ramasesha, J.-P. Sutter, *Chem. Commun.* **2015**, *51*, 3616.

[37] C. G. Werncke, P. C. Bunting, C. Duhayon, J. R. Long, S. Bontemps, S. Sabo-Etienne, *Angew. Chem. Int. Ed.* **2015**, *54*, 245; *Angew. Chem.* **2015**, *127*, 247.

[38] The Mössbauer spectrum recorded at 80 K (Figure S15) can be fitted as an asymmetric doublet with an isomer shift of $\delta = 0.72\ mm\,s^{-1}$ and a quadrupole splitting of $\Delta E_Q = 2.23\ mm\,s^{-1}$.[41] The obtained δ value is somewhat higher than the typical values for a few known two-coordinate Fe^I complexes (ca. 0.4 to $0.5\ mm\,s^{-1}$).[21–24,30,34] However, a value of $\delta = 0.81\ mm\,s^{-1}$ has also been reported,[35] indicating the high sensitivity of the Mössbauer parameter to the electronic and geometric effects of coordinating ligands.

[39] M. Atanasov, D. Ganyushin, K. Sivalingam, F. Neese in: *Molecular Electronic Structures of Transition Metal Complexes II* (Eds.: D. M. P. Mingos, P. Day, J. P. Dahl), Springer, Berlin, Heidelberg, **2012**, pp. 149.

[40] R. E. Cowley, E. Bill, F. Neese, W. W. Brennessel, P. L. Holland, *Inorg. Chem.* **2009**, *48*, 4828.

[41] P. Gütlich, E. Bill, A. X. Trautwein, *Mössbauer Spectroscopy and Transition Metal Chemistry*, Springer, Heidelberg, **2011**.

[42] R. L. Carlin, *Magnetochemistry*, Springer, Berlin, Heidelberg, **1986**.

[43] a) J. R. Vance, A. P. M. Robertson, K. Lee, I. Manners, *Chem. Eur. J.* **2011**, *17*, 4099; b) J. R. Vance, A. Schäfer, A. P. M. Robertson, K. Lee, J. Turner, G. R. Whittell, I. Manners, *J. Am. Chem. Soc.* **2014**, *136*, 3048.

[44] R. T. Baker, J. C. Gordon, C. W. Hamilton, N. J. Henson, P.-H. Lin, S. Maguire, M. Murugesu, B. L. Scott, N. C. Smythe, *J. Am. Chem. Soc.* **2012**, *134*, 5598.

[45] J. F. Sonnenberg, R. H. Morris, *ACS Catal.* **2013**, *3*, 1092.

[46] P. Bhattacharya, J. A. Krause, H. Guan, *J. Am. Chem. Soc.* **2014**, *136*, 11153.

[47] A. Glüer, M. Förster, V. R. Celinski, J. Schmedt auf der Günne, M. C. Holthausen, S. Schneider, *ACS Catal.* **2015**, *5*, 7214.

[48] a) C. Lichtenberg, M. Adelhardt, T. L. Gianetti, K. Meyer, B. de Bruin, H. Grützmacher, *ACS Catal.* **2015**, *5*, 6230; b) C. Lichtenberg, L. Viciu, M. Adelhardt, J. Sutter, K. Meyer, B. de Bruin, H. Grützmacher, *Angew. Chem. Int. Ed.* **2015**, *54*, 5766; *Angew. Chem.* **2015**, *127*, 5858.